



## The cost of toxin production in phytoplankton: the case of PST producing dinoflagellates

Chakraborty, Subhendu; Pani, Marina; Andersen, Ken Haste; Kiørboe, Thomas

*Published in:*  
I S M E Journal

*Link to article, DOI:*  
[10.1038/s41396-018-0250-6](https://doi.org/10.1038/s41396-018-0250-6)

*Publication date:*  
2019

*Document Version*  
Early version, also known as pre-print

[Link back to DTU Orbit](#)

*Citation (APA):*  
Chakraborty, S., Pani, M., Andersen, K. H., & Kiørboe, T. (2019). The cost of toxin production in phytoplankton: the case of PST producing dinoflagellates. *I S M E Journal*, 13(1), 64-75. <https://doi.org/10.1038/s41396-018-0250-6>

---

### General rights

Copyright and moral rights for the publications made accessible in the public portal are retained by the authors and/or other copyright owners and it is a condition of accessing publications that users recognise and abide by the legal requirements associated with these rights.

- Users may download and print one copy of any publication from the public portal for the purpose of private study or research.
- You may not further distribute the material or use it for any profit-making activity or commercial gain
- You may freely distribute the URL identifying the publication in the public portal

If you believe that this document breaches copyright please contact us providing details, and we will remove access to the work immediately and investigate your claim.

1    **Title of the paper: The cost of toxin production in phytoplankton: the case of**  
2    **PST producing dinoflagellates**

3    **Running title: Cost of toxin production**

4    Subhendu Chakraborty<sup>†</sup>, Marina Pančić, Ken H. Andersen, Thomas Kiørboe

5    Centre for Ocean Life, DTU Aqua, Technical University of Denmark, Kemitorvet,  
6    2800 Kgs. Lyngby, Denmark

7

8

9

10

11

12

13

14

15

16    <sup>†</sup>Corresponding author: Building 202, Centre for Ocean Life, DTU Aqua, Technical  
17    University of Denmark, Kemitorvet, 2800 Kgs. Lyngby, Denmark. Tel:  
18    +4591714664. Email: subc@aqua.dtu.dk

## **Abstract**

Many species of phytoplankton produce toxins that may provide protection from grazing. In that case one would expect toxin production to be costly; else all species would evolve toxicity. However, experiments have consistently failed to show any costs. Here, we show that costs of toxin production are environment dependent but can be high. We develop a fitness optimization model to estimate rate, costs, and benefits of toxin production, using PST (paralytic shellfish toxin) producing dinoflagellates as an example. Costs include energy and material (nitrogen) costs estimated from well-established biochemistry of PSTs, and benefits are estimated from relationship between toxin content and grazing mortality. The model reproduces all known features of PST production: inducibility in the presence of grazer cues, low toxicity of nitrogen-starved cells, but high toxicity of P- and light-limited cells. The model predicts negligible reduction in cell division rate in nitrogen replete cells, consistent with observations, but >20% reduction when nitrogen is limiting and abundance of grazers high. Such situation is characteristic of coastal and oceanic waters during summer when blooms of toxic algae typically develop. The investment in defense is warranted, since the net growth rate is always higher in defended than in undefended cells.

## **Key words**

Defense; Trade-off; Environment-dependent cost

## Introduction

Many phytoplankton species produce substances that are toxic to humans, hence we consider such phytoplankton ‘toxic algae’, but the evolution and functional role of these secondary metabolites remain unclear. They may be released into the environment and have allelochemical effects to combat competitors [1, 2] or grazers [3], they may be mainly intracellular and have toxic and/or deterrent effects on grazers [4, 5], or in mixotrophic species they may have offensive roles, functioning as a venom towards prey [6–8]. Some toxic algae may also form dense blooms, potentially promoted by their toxicity and consequent grazer deterrent effects, and a defensive role of toxin production is thus often assumed [4, 9]. This interpretation is supported by the observations that algal toxins often have a deterrent rather than a toxic effect on grazers [10–15], and that toxin production may be upregulated in the presence of grazers or their cues, as demonstrated in dinoflagellates, *Alexandrium* spp. [13, 16, 17], and in diatoms, *Pseudo-nitzschia* spp. [18]. The latter observation also suggests that toxin production comes at a cost – why else regulate the production in response to the need? Optimal defense theory, well founded in terrestrial plant ecology, predicts that inducibility of defense should evolve only when the defense is costly and variable in time [19]. However, experiments have generally been unable to demonstrate such costs in toxic phytoplankton, and the growth rates of grazer-induced and un-induced cells, or of toxic and nontoxic strains of the same phytoplankton species appear to be similar [3, 13, 16, 18], and model exercises have similarly suggested costs to be trivial [20]. However, if defense via toxin production is both effective and costless, one would expect most phytoplankton to be toxic, which is far from being the case [19]. Also, the promotion of phytoplankton diversity in the ocean due to grazing and consequent evolution of defense mechanisms, as demonstrated in

67 both theoretical models and considerations [21–23] and whole-community  
68 experiments [24], functions only if the defense comes at a cost.

69 One of the most studied groups of toxic phytoplankton is the dinoflagellate  
70 *Alexandrium* spp. since the toxins it produces, Paralytic Shellfish Toxins (PSTs), have  
71 serious effects on humans. The main potential grazers of dinoflagellates are copepods.  
72 While the toxin production may be induced by grazer (copepod) cues [13], the  
73 production also depends on the nutrient status of the algae. Specifically, when  
74 nitrogen or carbon (light) is limiting the PST production is reduced, while nutrient  
75 balanced or P-limited cells may produce PSTs at a high rate (growth of P-limited cells  
76 decreases while the production of toxins continues) [25, 26]. PSTs contain large  
77 amounts of nitrogen, and so this dependency suggests that the costs of PST  
78 production only become obvious when N or light is limiting, and may become  
79 manifest either as a reduction in growth rate because part of the assimilated N goes  
80 towards PST production; or as a cessation of the production of PSTs in favor of a  
81 higher growth rate with a consequent loss of the defense; or a combination of the two.

82 Here, we explore by means of a simple resource allocation model the costs of  
83 chemical defense in phytoplankton, using PST producing dinoflagellate *Alexandrium*  
84 spp. as an example. We consider both energy and material costs of PST production,  
85 their dependency on environmental conditions, and the reduction in mortality that is  
86 achieved by the defense investments. Through fitness optimization we demonstrate  
87 that costs can be substantial, leading to > 20% reduction in cell division rate, when  
88 grazer abundance is high and nitrogen availability is low. We also examine the  
89 conditions under which the production of toxins provides maximum benefit to the  
90 toxin producing species.

## 91 **Model description:**

92 The model is based on a resource allocation optimization model modified from Berge  
93 *et al.* [27]. The division rate of phytoplankton depends on the acquisition of three  
94 resources, viz. carbon (via photosynthesis), nitrogen (as nitrate), and phosphorous (as  
95 phosphate), as well as on metabolic expenses. The cells may invest some of their  
96 assimilated nitrogen into toxin production and combust some of their fixed organic  
97 carbon to cover costs of toxin synthesis, and in return experience reduced grazing  
98 mortality. We search for the investment that maximizes the fitness of the cells,  
99 defined as the difference between cell division rate and mortality rate (= net growth  
100 rate). We use the model to explore the dependency of division rate, net growth rate,  
101 and toxicity on the environmental resource availability and predation risk.

102 Uptake of carbon, nitrogen and phosphorous to the cell is described by the symbol  $J_i$   
103 (mass flows  $i$  being carbon via light-dependent photosynthesis (C), nitrogen (N) or  
104 phosphorous (P) in units of  $\mu\text{g}$  per day; see Table 1 for central symbols and  
105 parameters), and are combined to synthesize new biomass (Fig. 1). Respiratory costs,  
106  $R_C$  (units of  $\mu\text{g}$  C per day), include costs of biomass synthesis (incl. transport) and  
107 maintenance of the structure. Toxin is produced at a rate,  $T_r$ , and implies an additional  
108 respiratory cost,  $R_T$ . Biomass synthesis rate,  $J_{tot}$ , is constrained by the stoichiometric  
109 balance between carbon, nitrogen and phosphorous. Finally, we assume that toxins  
110 and structure have constant but different stoichiometry.

### 111 *Uptake of carbon, nitrogen, and phosphorous*

112 The potential uptake  $J_i$  of resource  $i$  (C, N, P) is governed by a standard saturating  
113 functional response:

$$J_i = M_i \frac{A_i Y_i}{A_i Y_i + M_i}, (1)$$

114 where  $A_i$  is the affinity for resource  $i$ ,  $Y_i$  resource concentration ( $\mu\text{g L}^{-1}$ ), and  $M_i$  is  
115 the maximum uptake rate.

#### 116 *Costs*

117 Respiratory costs include costs of both uptake and mobilization of resources for  
118 synthesis through each pathway, and the maintenance of the structure. This metabolic  
119 cost is assumed to be 30% of the total carbon budget [28] plus a constant basal  
120 respiration ( $R_0$ ) independent of  $J_C$ , i.e.,

$$R_C = 0.3J_C + R_0. (2)$$

#### 121 *Rate and cost of toxin production*

122 Let  $\theta$  be the fraction of nitrogen uptake that a toxic phytoplankton cell devotes to  
123 toxin production. Then the potential rate of toxin production is (units of  $\mu\text{g N d}^{-1}$ ):

$$124 \quad T_{pot}(\theta) = \theta J_N. \quad (3)$$

125 As the toxin production needs carbon both for building the toxin molecules and to  
126 fuel the respiratory costs of toxin production, the actual toxin production rate may be  
127 limited by the available carbon to:

$$128 \quad T_r(\theta) = \min[T_{pot}(\theta), (J_C - R_C)/(n_T + r_T)], (4)$$

129 where  $n_T$  is the mass of carbon need per mass of nitrogen in the toxin, and  $r_T$  is the  
130 respiratory cost per nitrogen synthesized into toxins (units of  $\text{g C (g N)}^{-1}$ ).

131 The total cost of toxin production in terms of carbon then becomes ( $\mu\text{g C d}^{-1}$ ):

132 
$$R_T(\theta) = (n_T + r_T)T_r(\theta). \quad (5)$$

133 *Synthesis and growth rate*

134 The assimilated carbon, nitrogen and phosphorous are combined to synthesize new  
135 structure. We assume constant C:N mass ratio,  $Q_{CN}$  (units of  $\mu\text{g C } (\mu\text{g N})^{-1}$ ) and C:P  
136 mass ratio,  $Q_{CP}$  (units of  $\mu\text{g C } (\mu\text{g P})^{-1}$ ) of the cell. The total available carbon for  
137 growth is then  $J_C - R_C - R_T$  where  $J_C$  represents the total uptake of carbon through  
138 photosynthesis, and  $R_C$  and  $R_T$  represent the costs of maintenance and biomass  
139 synthesis, and costs of toxin production, respectively. The carbon required to  
140 synthesize biomass from nutrients is  $Q_{CN}(J_N - T_r)$  and  $Q_{CP}J_P$  for nitrate and  
141 phosphate, respectively. The growth rate is constrained by the limiting resource  
142 (Liebig's law of the minimum) such that the total flux of carbon (and nutrients)  
143 available for growth  $J_{\text{tot}}$  is:

$$J_{\text{tot}}(\theta) = \min[J_C - R_C - R_T(\theta), Q_{CN}(J_N - T_r(\theta)), Q_{CP}J_P]. \quad (6)$$

144 Synthesis is not explicitly limited by a maximum synthesis capacity; limitation of  
145 synthesis is taken care of by the limitation of uptake of carbon, nitrogen and  
146 phosphorous in the functional responses (Eq. 1). The division rate  $\mu$  of the cells ( $\text{d}^{-1}$ )  
147 is the total flux of carbon divided by the carbon mass of the cell ( $w_X$ ):

148 
$$\mu(\theta) = J_{\text{tot}}(\theta)/w_X. \quad (7)$$

149 Further subtracting the predation mortality ( $m_p$ ) yields the net growth rate ( $r$ ):

150 
$$r(\theta) = \mu(\theta) - m_p(\theta). \quad (8)$$



151 We assume that predation mortality increases linearly with zooplankton biomass ( $Z$ ),  
 152 and due to the toxin production, zooplankton reduces its grazing pressure on toxic  
 153 cells exponentially as:

$$154 \quad m_p(\theta) = m_{p,0} Z e^{-\beta T(\theta)}, \quad (9)$$

155 where  $m_{p,0}$  is a mortality constant,  $T$  is the cellular toxin content ( $\mu\text{g N cell}^{-1}$ )  
 156 estimated as the toxin production rate divided by the cell division rate ( $= T_r/\mu$ ), and  
 157  $\beta$  represents the strength of toxic effect.

158 The resulting population growth rate,  $r(\theta)$ , is a measure of the fitness of the  
 159 phytoplankton and we assume that the cell has the ability to optimize its growth rate  
 160 by regulating its resource allocation to toxin production such that it maximizes its  
 161 fitness. The optimal proportion of assimilated N devoted to toxin production then  
 162 becomes:

$$163 \quad \theta^* = \operatorname{argmax}_{\theta} \{r(\theta)\}. \quad (10)$$

## 164 **Model parameterization**

165 Calibration of parameters is based on laboratory measurements on the dinoflagellates  
 166 *Alexandrium minutum* and *A. tamarense* as the toxic species, and the copepods  
 167 *Acartia clausi* and *A. tonsa* as the grazer zooplankton. To calibrate the basic grazing  
 168 parameters, we use data for non-toxic strains of *A. minutum*.

169 *Parameters related to phytoplankton division rate ( $\mu$ ):*

170 We use experimental observations reported in the literature for cell division rate ( $\mu$ )  
 171 of *A. minutum* as a function of light intensity ( $L$ ) and nutrient concentrations ( $N$  and

P) to estimate parameter values for maximum uptake rates ( $M_i$ ) and affinities ( $A_i$ ) (Fig. 2a-c). While calibrating these parameters a non-toxic strain of *A. minutum* was considered, and as a result, no cost is deducted. For calibration, we adjust the parameters manually to fit the curves with data and keep them close to the existing values of the parameters from other studies (when available). Due to Liebig's minimum law for synthesis (eq. 6), the synthesis is limited by one of the resources (either C or N) and further growth cannot materialize in spite of the availability of other non-limiting resource. As a result, growth cannot increase any further.

We use a constant value  $1.07 \times 10^{-4} \mu\text{g C d}^{-1}$  for the basal respiration rate ( $R_0$ ) taken from the range reported in Frangoulis *et al.* [29].

#### *Parameters related to the cost of toxin production:*

To estimate the two parameters related to the cost of toxin production ( $n_T$ ,  $r_T$ ), we consider the stoichiometry of PSTs and the biochemistry of PST synthesis. PSTs produced by *Alexandrium* spp. (and other organisms) consist of saxitoxin and multiple derivatives; they are cyclic nitrogenous compounds that are synthesized from amino acid precursors. Here we consider the synthesis of saxitoxin, one of the dominating toxins, from the amino acid glutamate via arginine to estimate the approximate costs of toxin production. The costs are two-fold; i.e. the metabolic cost of biosynthesis,  $r_T$ , and the cost in terms of material invested in the toxin,  $n_T$ .

*Material investment ( $n_T$ ):* The molecular formula of saxitoxin is  $\text{C}_{10}\text{H}_{17}\text{N}_7\text{O}_4$ , that is 10 moles of carbon per 7 moles of nitrogen, or  $n_T = (10 \times 12) / (7 \times 14) = 1.23 \mu\text{g C } (\mu\text{g N})^{-1}$ .

*Metabolic expenses* ( $r_T$ ): Saxitoxin is synthesized from arginine [30], which in turn is typically synthesized from glutamate that in phytoplankton has to be synthesized *de novo*. The metabolic cost of converting glutamate to arginine is 12 mol ATP per mol of arginine, and the synthesis of arginine precursors (i.e. glutamate and carbamoyl-P) requires another 32 mol of ATP, i.e. a total of 44 mol ATP per mol of arginine [31]. We have no estimate of the cost of synthesizing saxitoxin from arginine (e.g., necessary transcripts and translation to enzymes) as well as costs due to actual or potential autotoxicity (hence we ignore it), but it takes 3 mol of arginine to synthesize one mol of saxitoxin. Therefore, it requires at least 132 mol of ATP to synthesize 1 mol of saxitoxin. The respiratory equivalent of ATP synthesis is about 0.235 mol ATP synthesized per liter of oxygen consumed; or about 2 g of organic carbon combusted per mol of ATP synthesized [32]. Thus, 2x132 g of organic carbon is respired per mol of toxin synthesized. With 7x14 g N per mol toxin yields an estimate of  $r_T = 2.7 \mu\text{g C} (\mu\text{g N})^{-1}$ .

#### *Parameters related to zooplankton feeding:*

The parameters related to reduction in feeding on toxic cell ( $\beta$ ) was calibrated from Teegarden & Cembella [12] who quantified the feeding rate on a toxic strain of *A. minutum* by *A. tonsa* as a function of cellular toxin content ( $\mu\text{g N cell}^{-1}$ ). We fit Eq. 9 to the experimental data to estimate  $\beta$  (Fig. 2d). We use  $8.95 \times 10^{-4} \mu\text{g C}$  as the cellular carbon content of *A. minutum* [28], and chose the value of the mortality constant ( $m_{p,0}$ ) as  $0.008 \text{ L } (\mu\text{g C})^{-1} \text{ d}^{-1}$  based on the clearance rate of *A. tonsa* [34].

## **Results**

## 217 *Optimal allocation strategy*

218 The optimal allocation of nitrogen to toxin production is the one that yields the  
219 highest population growth rate (Fig. 3). The optimal allocation of N to toxin  
220 production increases with decreasing environmental nitrogen availability and  
221 increasing concentration of zooplankton (Fig. 3). As a result, the investment in  
222 defense - toxin production - in toxic dinoflagellates varies with both N-availability  
223 and grazing pressure, with implications to cell division rate, grazing mortality rate,  
224 and population growth rate (Fig. 4, Fig. 5, Fig. 6 and Fig. 7).

## 225 *Toxin production, grazing mortality, and cost of defense*

226 At high N concentrations, the cells produce toxin whenever zooplankton is present but  
227 production ceases in the absence of grazers (Fig. 4a). Note that for simplicity we  
228 assume that toxin production rate becomes zero when there is no grazer. In contrast,  
229 at low N, phytoplankton produce toxins only when zooplankton biomass exceeds a  
230 threshold concentration, and the cellular toxin content increases with the biomass of  
231 the zooplankton (Fig. 4a, 6b).

232 Defended cells experience lower grazing mortality than undefended cells especially  
233 when nitrogen availability is high and zooplankton concentration is low (Fig. 4d) as  
234 cellular toxin content remains high (Fig. 4a). Taken together the grazing mortality  
235 increases with zooplankton density and decreases with availability of nitrogen.

236 The cost of the defense can be quantified as a reduction in the cell division rate of  
237 defended relative to undefended cells. This cost is significant only at high  
238 zooplankton biomass and/or low nitrogen availability (Fig. 4b, Fig. 5a) and increases  
239 with increasing zooplankton biomass and decreasing nitrogen concentration (Fig. 6c,

d). At realistically high zooplankton biomass and realistically low nitrogen availability, cell division rate may be reduced by more than 20%. At high nitrogen concentrations, the cells produce toxins from the excess nitrogen (not used for growth) and therefore the costs are, of course, unmeasurably low (Fig. 6d). The net outcome of the defense investment is that defended cells have similar or higher population growth rates (fitness) than undefended cells under all nutrient conditions (Fig. 4c). The absolute enhancement is largest at high N (Fig. 6e) whereas the relative advantage is most pronounced at low N and high zooplankton biomass (Fig. 6f).

#### *Effects of P and light limitation*

If phosphate or light rather than nitrogen limit cell growth, N is in excess and the excess N can be allocated to toxin production and the cells consequently become well defended. Figs. 7a and b display the effects of light limitation on toxin production and cellular toxin contents, respectively. There are two regions in this parameter space: the left region where light is limiting and toxin production increases with light intensity while toxin content decreases with light intensity; and the right region, where nitrogen is limiting and both toxin production and cellular toxin content are independent of light intensity. Toxin production and cellular contents similarly vary in the nitrogen-phosphorous parameter space, between phosphorous limitation at low P and nitrogen limitation at high P (Fig. 7c, d). Under all conditions, cellular toxin contents increase with decreasing ambient P.

#### *Sensitivity analysis of $\beta$ and $r_T$*

Since the parameter  $\beta$  was calibrated based on only four available data points (Figure 2d), we perform a sensitivity analysis by varying  $\beta$ , which represents the reduction in

263 zooplankton grazing due to cellular toxin (see supplementary material fig. A1).  
264 Overall, the qualitative patterns described above are robust to changes in  $\beta$ . When  
265 nitrogen concentrations are high, there is no observable change in cellular toxin  
266 concentration with varying  $\beta$  as organisms produce toxins at their maximum rate and  
267 consequently division rates remain same. However, due to the increase in predation  
268 pressure with decreasing  $\beta$ , population growth rate decreases. On the other hand, with  
269 decrease in nitrogen concentrations, organisms produce more toxin with decrease in  
270  $\beta$ , leading to reduction in division rates as well as growth rates.

271 Similarly, varying the parameter  $r_T$ , representing the metabolic cost of synthesizing  
272 toxin, does not lead to observable changes in the system dynamics (see supplementary  
273 material fig. A2).

## 274 **Discussion**

275 Experiments have demonstrated that PST producing dinoflagellates become less toxic  
276 when N-starved, that toxin content is high in exponentially growing cells in N:P  
277 balanced environments, and that the cells become most toxic when P-limited [20, 26,  
278 35–37]. Light-limited cells also accumulate more toxins [38] and toxin production is  
279 enhanced in the presence of grazer cues [13]. Our model qualitatively reproduces all  
280 these observations.

281 The model further conforms with the experimental observation that the cost of toxin  
282 production, quantified as a reduction in cell division rate of toxin-producing cells  
283 compared to cells or strains that produce less or no toxins, is negligible when  
284 resources, mainly N and light, are plentiful [3, 13]. However, when light or nitrogen  
285 are limiting cell growth, and when grazers are abundant, we predict that the cost of

investing in toxin production may be substantial and lead to > 20% reduction in cell division rate. There is evidence for other defense mechanisms in phytoplankton where the cost of the defense only materializes when resources are limiting [39–41]. However, the prediction of costs of toxin production still remains to be tested experimentally. The costs of the investment are two-fold: (i) the cells need nitrogen to build toxin molecules, and this requirement compete with the nitrogen investment in cell structure and growth. While the nitrogen requirement for toxin production is small in absolute terms, leading John and Flynn [20] to consider it trivial, it becomes significant when nitrogen is limiting, and may eventually lead to a total shut down of toxin production. (ii) The cells further need energy for the synthesis of toxins, and this energy eventually comes from photosynthesis. This is why toxin production rate increases with light intensity when light is the limiting resource. In this situation, cell division rate increases faster than toxin production rate with increasing light, and therefore cellular toxin content decreases with increasing light, an effect and a mechanism in agreement with experimental observations [38].

The environmental conditions that promote cell toxicity, i.e., high grazer biomass, actually coincide with the time of the year when nitrogen is the most limiting resource in temperate shelf regions. Thus, zooplankton (copepod) biomass is at its seasonal maximum during summer and may easily exceed  $10\text{--}100\ \mu\text{g C L}^{-1}$  [42], which will impose a high predation mortality and thus induce high cell toxicity. At this time of the year, concentrations of inorganic nitrogen in surface waters in temperate shelf regions are low, typically below  $1\text{--}10\ \mu\text{g N L}^{-1}$  [43, 44], and under these conditions the model predicts that the cost of toxin production is substantial, leading to > 20% decrease in cell division rate. However, the investment in defense pays off since defended cells experience lower grazing mortality, and may consequently have net

growth rates up to twice or more of that of undefended cells (e.g. Fig. 6f). If the toxins have deterrent rather than toxic effects, i.e., preventing the toxic cells from being consumed rather than killing grazers that do consume the cells [10, 11, 45], then the toxic cells may have a competitive advantage and a monospecific bloom may develop. Indeed, blooms of toxic algae typically occur during summer [46], which is consistent with these considerations.

Furthermore, the toxic species can also gain growth advantage under high nitrogen and high grazer biomass, as growth rates can be doubled due to the benefit provided by toxin production at a negligible production cost (Fig. 6d, f). Such situations are comparable with many coastal areas where N:P ratios remain considerably high due to erratic input of nitrogen from human activities, and can consequently result in toxic blooms [47]. Thus, potentially toxic species can also become toxic when exposed to high N regime caused by eutrophication.

The success of toxic bloom formation also depends on the evolutionary history of zooplankton grazer and toxic species [40]. Evidence from both fresh- and marine waters shows that grazers can evolve full or partial resistance against the toxic algae [48, 49]. Our results suggest that cellular toxin content will increase in the presence of toxin-resistant grazers as will the costs (see supplementary material fig. A1). However, if the benefits in terms of reduced grazing mortality vanish due to grazer resistance, the possibility of success of the toxic species in terms of forming bloom will be reduced or disappear.

Many phytoplankton species have evolved what is supposed to be defense mechanisms to avoid or reduce predation, ranging from hard shells and spines, to evasive behaviors and toxin production, and such defenses may have significant



implications on predator-prey interactions, population dynamics, and diversity of phytoplankton communities [50]. However, the trade-offs are rarely quantified and often not even documented. While there is increasing evidence that toxin-production in many cases provides partial protection from grazing in dinoflagellates, the costs have hitherto not been properly quantified. The currencies of benefits and costs are growth and mortality. Here, we have shown that the costs are not only strongly dependent on the concentration of grazers but also on the resource availability, and that the realized costs in nature are typically highest during summer when the defense is most needed. The delicate balance between costs, benefits, and resource availability not only explains why the defense is inducible but also has implications for the timing of toxic algal blooms. Further studies on costs and benefits of toxin production are needed to experimentally test our model predictions (e.g., toxin production and growth under sufficient and deficient resources), and for deeper understanding of the mechanisms and evolution of inducible toxin production. At present, very little is known about the consequences of inducible toxin production on the community level in complex communities. Future work should be devoted towards investigating the complex integrated ecological issues of inducible toxin production, species diversity, and food web structure.

### **Acknowledgments**

The Centre for Ocean Life is supported by the Villum Foundation. S.C. was supported by the H. C. Ørsted COFUND postdoc fellowship and additional support was received from the Gordon & Betty Moore Foundation through award #5479.

### **Conflict of interest**

The authors declare that they have no conflict of interest.

## 359    **References**

- 360    1.    Blossom HE, Andersen NG, Rasmussen SA, Hansen PJ. Stability of the intra-  
361            and extracellular toxins of *Prymnesium parvum* using a microalgal bioassay.  
362            *Harmful Algae* 2014; **32**: 11–21.
- 363    2.    Legrand C, Rengefors K, Fistarol GO, Granéli E. Allelopathy in phytoplankton  
364            - biochemical, ecological and evolutionary aspects. *Phycologia* 2003; **42**: 406–  
365            419.
- 366    3.    John U, Tillmann U, Hülskötter J, Alpermann TJ, Wohlrab S, Van De Waal  
367            DB. Intraspecific facilitation by allelochemical mediated grazing protection  
368            within a toxigenic dinoflagellate population. *Proc R Soc B Biol Sci* 2015; **282**:  
369            1–9.
- 370    4.    Turner JT. Planktonic marine copepods and harmful algae. *Harmful Algae*  
371            2014; **32**: 81–93.
- 372    5.    Colin SP, Dam HG. Effects of the toxic dinoflagellate *Alexandrium fundyense*  
373            on the copepod *Acartia hudsonica*: A test of the mechanisms that reduce  
374            ingestion rates. *Mar Ecol Prog Ser* 2003; **248**: 55–65.
- 375    6.    Driscoll WW, Hackett JD, Ferrière R. Eco-evolutionary feedbacks between  
376            private and public goods: Evidence from toxic algal blooms. *Ecol Lett* 2016;  
377            **19**: 81–97.
- 378    7.    Blossom HE, Daugbjerg N, Hansen PJ. Toxic mucus traps: A novel mechanism  
379            that mediates prey uptake in the mixotrophic dinoflagellate *Alexandrium*  
380            pseudogonyaulax. *Harmful Algae* 2012; **17**: 40–53.

- 381 8. Sheng J, Malkiel E, Katz J, Adolf JE, Place AR. A dinoflagellate exploits  
382 toxins to immobilize prey prior to ingestion. *Proc Natl Acad Sci* 2010; **107**:  
383 2082–2087.
- 384 9. Wolfe G V. The chemical defense ecology of marine unicellular plankton:  
385 Constraints, mechanisms, and impacts. *Biol Bull* 2000; **198**: 225–244.
- 386 10. Xu J, Nielsen LT, Kiørboe T. Foraging response and acclimation of ambush  
387 feeding and feeding-current feeding copepods to toxic dinoflagellates. *Limnol*  
388 *Oceanogr* 2018.
- 389 11. Xu J, Hansen JP, Nielsen TL, Krock B, Tillmann U, Kiørboe T. Distinctly  
390 different behavioral responses of a copepod, *Temora longicornis*, to different  
391 strains of toxic dinoflagellates, *Alexandrium* spp. *Harmful Algae* 2017; **62**: 1–  
392 9.
- 393 12. Teegarden GJ, Cembella AD. Grazing of toxic dinoflagellates, *Alexandrium*  
394 spp, by adult copepods of coastal Maine: Implications for the fate of paralytic  
395 shellfish toxins in marine food webs. *J Exp Mar Bio Ecol* 1996; **196**: 145–176.
- 396 13. Selander E, Thor P, Toth G, Pavia H. Copepods induce paralytic shellfish toxin  
397 production in marine dinoflagellates. *Proc R Soc B Biol Sci* 2006; **273**: 1673–  
398 1680.
- 399 14. Schultz M, Kiørboe T. Active prey selection in two pelagic copepods feeding  
400 on potentially toxic and non-toxic dinoflagellates. *J Plankton Res* 2009; **31**:  
401 553–561.
- 402 15. Sykes PF, Huntley ME. Acute physiological reactions of *Calanus pacificus* to

- 403 selected dinoflagellates: Direct observations. *Mar Biol* 1987; **94**: 19–24.
- 404 16. Selander E, Fagerberg T, Wohlrab S, Pavia H. Fight and flight in  
 405 dinoflagellates? Kinetics of simultaneous grazer-induced responses in  
 406 *Alexandrium tamarense*. *Limnol Oceanogr* 2012; **57**: 58–64.
- 407 17. Senft-Batoh CD, Dam HG, Shumway SE, Wikfors GH. A multi-phylum study  
 408 of grazer-induced paralytic shellfish toxin production in the dinoflagellate  
 409 *Alexandrium fundyense*: A new perspective on control of algal toxicity.  
 410 *Harmful Algae* 2015; **44**: 20–31.
- 411 18. Harðardóttir S, Pančić M, Tammilehto A, Krock B, Møller EF, Nielsen TG, et  
 412 al. Dangerous relations in the Arctic marine food web: Interactions between  
 413 toxin producing *Pseudo-nitzschia* diatoms and *Calanus* copepodites. *Mar*  
 414 *Drugs* 2015; **13**: 3809–3835.
- 415 19. Karban R. The ecology and evolution of induced resistance against herbivores.  
 416 *Funct Ecol* 2011; **25**: 339–347.
- 417 20. John EH, Flynn KJ. Modelling changes in paralytic shellfish toxin content of  
 418 dinoflagellates in response to nitrogen and phosphorus supply. *Mar Ecol Prog*  
 419 *Ser* 2002; **225**: 116–147.
- 420 21. Thingstad TF, Våge S, Storesund JE, Sandaa R-A, Giske J. A theoretical  
 421 analysis of how strain-specific viruses can control microbial species diversity.  
 422 *Proc Natl Acad Sci* 2014; **111**: 7813–7818.
- 423 22. Våge S, Storesund JE, Giske J, Thingstad TF. Optimal defense strategies in an  
 424 idealized microbial food web under trade-off between competition and defense.

425 *PLoS One* 2014; **9**.

426 23. Strauss SY, Rudgers JA, Lau JA, Irwin RE. Direct and ecological costs of  
 427 resistance to herbivory. *Trends Ecol Evol* 2002; **17**: 278–285.

428 24. Leibold MA, Hall SR, Smith VH, Lytle DA. Herbivory enhances the diversity  
 429 of primary producers in pond ecosystems. *Ecology* 2017; **98**: 48–56.

430 25. Anderson DM, Kulis DM, J.J. S, Hall S, Lee C. Dynamics and physiology of  
 431 saxitoxin production by the dinoflagellate *Alexandrium* spp. *Mar Biol* 1990;  
 432 **104**: 511–524.

433 26. John EH, Flynn KJ. Growth dynamics and toxicity of *Alexandrium fundyense*  
 434 (Dinophyceae): The effect of changing N:P supply ratios on internal toxin and  
 435 nutrient levels. *Eur J Phycol* 2000; **35**: 11–23.

436 27. Berge T, Chakraborty S, Hansen PJ, Andersen KH. Modeling succession of  
 437 key resource-harvesting traits of mixotrophic plankton. *ISME J* 2017; **11**: 212–  
 438 223.

439 28. López-Sandoval DC, Rodríguez-Ramos T, Cermeño P, Sobrino C, Marañón E.  
 440 Photosynthesis and respiration in marine phytoplankton: Relationship with cell  
 441 size, taxonomic affiliation, and growth phase. *J Exp Mar Bio Ecol* 2014; **457**:  
 442 151–159.

443 29. Frangoulis C, Carlotti F, Eisenhauer L, Zervoudaki S. Converting copepod  
 444 vital rates into units appropriate for biogeochemical models. *Prog Oceanogr*  
 445 2010; **84**: 43–51.

446 30. Kellmann R, Mihali TK, Young JJ, Pickford R, Pomati F, Neilan BA.

- 447 Biosynthetic intermediate analysis and functional homology reveal a saxitoxin  
448 gene cluster in cyanobacteria. *Appl Environ Microbiol* 2008; **74**: 4044–4053.
- 449 31. Atkinson DE. Cellular Energy Metabolism and Its Regulation. 1977. Academic  
450 Press.
- 451 32. Kiørboe T, Møhlenberg F, Hamburger K. Bioenergetics of the planktonic  
452 copepod *Acartia tonsa*: Relation between feeding, egg production and  
453 respiration, and composition of specific dynamic action. *Mar Ecol Prog Ser*  
454 1985; **26**: 85–97.
- 455 34. Saiz E, Kiørboe T. Predatory and suspension feeding of the copepod *Acartia*  
456 *tonsa* in turbulent environments. *Mar Ecol Prog Ser* 1995; **122**: 147–158.
- 457 35. Boyer GL, Sullivan JJ, Andersen RJ, Harrison PJ, Taylor FJR. Effects of  
458 nutrient limitation on toxin production and composition in the marine  
459 dinoflagellate *Protogonyaulax tamarens*. *Mar Biol* 1987; **128**: 123–128.
- 460 36. Han M, Lee H, Anderson DM, Kim B. Paralytic shellfish toxin production by  
461 the dinoflagellate *Alexandrium pacificum* (Chinhae Bay, Korea) in axenic,  
462 nutrient-limited chemostat cultures and nutrient-enriched batch cultures. *Mar*  
463 *Pollut Bull* 2016; **104**: 34–43.
- 464 37. Murata A, Nagashima Y, Taguchi S. N:P ratios controlling the growth of the  
465 marine dinoflagellate *Alexandrium tamarens*: Content and composition of  
466 paralytic shellfish poison. *Harmful Algae* 2012; **20**: 11–18.
- 467 38. Ogata T, Ishimura T, Kodama M. Effect of water temperature and light  
468 intensity on growth rate and toxicity change in *Protogonyaulax tamarens*.

- 469 *Mar Biol* 1987; **95**: 217–220.
- 470 39. Zhu X, Wang J, Chen Q, Chen G, Huang Y, Yang Z. Costs and trade-offs of  
 471 grazer-induced defenses in *Scenedesmus* under deficient resource. *Sci Rep*  
 472 2016; **6**: 1–10.
- 473 40. Yoshida T, Hairston NG, Ellner SP. Evolutionary trade-off between defence  
 474 against grazing and competitive ability in a simple unicellular alga, *Chlorella*  
 475 *vulgaris*. *Proc R Soc B-Biological Sci* 2004; **271**: 1947–1953.
- 476 41. Yoshida T, Jones LE, Ellner SP, Fussmann GF, Hairston NG. Rapid evolution  
 477 drives ecological dynamics in a predator – prey system. *Nature* 2003; **424**:  
 478 303–306.
- 479 42. Kiørboe T, Nielsen TG. Regulation of zooplankton biomass and production in  
 480 a temperate, coastal ecosystem. 1. Copepods. *Limnol Ocean* 1994; **39**: 493–  
 481 507.
- 482 43. Andersson L. Trends in nutrient and oxygen concentrations in the Skagerrak-  
 483 Kattegat. *J Sea Res* 1996; **35**: 63–71.
- 484 44. Brockmann UW, Topcu DH. Nutrient atlas of the central and northern North  
 485 Sea. 2002. Federal Environmental Agency, Berlin, Germany.
- 486 45. Teegarden GJ. Copepod grazing selection and particle discrimination on the  
 487 basis of PSP toxin content. *Mar Ecol Prog Ser* 1999; **181**: 163–176.
- 488 46. Heisler J, Glibert PM, Burkholder JM, Anderson DM, Cochlan W, Dennison  
 489 WC, et al. Eutrophication and harmful algal blooms: A scientific consensus.  
 490 *Harmful Algae* 2008; **8**: 3–13.

- 491 47. Hallegraeff GM. A review of harmful algal blooms and their apparent global  
492 increase. *Phycologia* 1993; **32**: 79–99.
- 493 48. Gilbert JJ. Differential effects of *Anabaena affinis* on Cladocerans and  
494 Rotifers: Mechanisms and implications. *Ecology* 1990; **71**: 1727–1740.
- 495 49. Colin SP, Dam HG. Latitudinal differentiation in the effects of the toxic  
496 dinoflagellate *Alexandrium* spp. on the feeding and reproduction of  
497 populations of the copepod *Acartia hudsonica*. *Harmful Algae* 2002; **1**: 113–  
498 125.
- 499 50. Pančić M, Kiørboe T. Phytoplankton defence mechanisms: Traits and trade-  
500 offs. *Biol Rev* 2018.
- 501 51. Redfield AC. The biological control of chemical factors in the environment.  
502 *Am Sci* . 1958. Sigma Xi, The Scientific Research Honor Society. , **46**: 205–  
503 221
- 504 52. Chang FH, McClean M. Growth responses of *Alexandrium minutum*  
505 (*Dinophyceae*) as a function of three different nitrogen sources and irradiance.  
506 *New Zeal J Mar Freshw Res* 1997; **31**: 1–7.
- 507 53. Ignatiades L, Gotsis-Skretas O, Metaxatos A. Field and culture studies on the  
508 ecophysiology of the toxic dinoflagellate *Alexandrium minutum* (Halim)  
509 present in Greek coastal waters. *Harmful Algae* 2007; **6**: 153–165.
- 510 54. Lim PT, Leaw CP, Usup G, Kobiyama A, Koike K, Ogata T. Effects of light  
511 and temperature on growth, nitrate uptake, and toxin production of two tropical  
512 dinoflagellates: *Alexandrium tamiyavanichii* and *Alexandrium minutum*



513 (Dinophyceae). *J Phycol* 2006; **42**: 786–799.

514

515

516

517

518

519

520

521

522

523

524

525

526

527

528

529

530 **Table 1.** Central symbols and general parameters. Index  $i$  refers to carbon ( $C$ ) via  
531 light-dependent photosynthesis where light intensity is measured in units of  
532  $\mu\text{E m}^{-2}\text{s}^{-1}$ , nitrogen ( $N$ ) in units of  $\mu\text{g N L}^{-1}$  or phosphorous (P) in units of  $\mu\text{g P L}^{-1}$ .  
533 Calibration of parameters is based on data from laboratory measurements and  
534 provided in the ‘Model parameterization’ section.

Symbol	Description	Value	Unit	Reference
--------	-------------	-------	------	-----------

---

L	Light flux in the environment	-	$\mu\text{E m}^{-2}\text{s}^{-1}$	-
N	Concentration of nitrogen in the environment	-	$\mu\text{g N L}^{-1}$	-
P	Concentration of phosphorous in the environment	-	$\mu\text{g P L}^{-1}$	-
$w_X$	Cellular mass of toxic algae	$8.95 \times 10^{-4}$	$\mu\text{g C}$	[28]
Z	Biomass of zooplankton	-	$\mu\text{g C L}^{-1}$	-
<b>Functional responses</b>				
$J_i$	Flux of assimilated substance		$\mu\text{g C d}^{-1}, \mu\text{g N d}^{-1}, \text{ or } \mu\text{g P d}^{-1}$	Eq. (1)
$A_L$	Affinity for light	$3.1 \times 10^{-5}$	$\mu\text{g C } (\mu\text{E m}^{-2}\text{s}^{-1})^{-1} \text{ d}^{-1}$	Calibrated
$A_N$	Affinity for nitrogen	$3 \times 10^{-6}$	$\text{L d}^{-1}$	Calibrated
$A_P$	Affinity for phosphorous	$3 \times 10^{-7}$	$\text{L d}^{-1}$	Calibrated
$M_L$	Max. uptake rate of C through photosynthesis	$9.5 \times 10^{-4}$	$\mu\text{g C d}^{-1}$	Calibrated
$M_N$	Max. uptake rate of N	$1.1 \times 10^{-4}$	$\mu\text{g N d}^{-1}$	Calibrated
$M_P$	Max. uptake rate of P	$1.3 \times 10^{-5}$	$\mu\text{g P d}^{-1}$	Calibrated
<b>Costs and toxin production</b>				
$R_C$	Total metabolic cost	-	$\mu\text{g C d}^{-1}$	Eq. (2)
$R_0$	Basal respiration rate	$1.07 \times 10^{-4}$	$\mu\text{g C d}^{-1}$	[29]
$\theta$	Fraction of N devoted to toxin	-	-	Eq. (10)
$T_{pot}$	Potential toxin production rate	-	$\mu\text{g N d}^{-1}$	Eq. (3)
$T_r$	Actual toxin production rate	-	$\mu\text{g N d}^{-1}$	Eq. (4)
T	Cellular toxin content	-	$\mu\text{g N cell}^{-1}$	-
$R_T$	Cost of toxin production	-	$\mu\text{g C d}^{-1}$	Eq. (5)
$n_T$	Material cost of toxin production	1.23	$\mu\text{g C } (\mu\text{g N})^{-1}$	Calibrated
$r_T$	Metabolic cost of synthesizing toxin	2.7	$\mu\text{g C } (\mu\text{g N})^{-1}$	Calibrated
<b>Predation</b>				
$m_p$	Predation mortality	-	$\text{d}^{-1}$	Eq. (9)

$m_{p,0}$	Mortality constant	0.008	$L (\mu g C)^{-1} d^{-1}$	[34]
$\beta$	Reduction in grazing due to toxin	$1.147 \times 10^5$	cells $(\mu g N)^{-1}$	Calibrated
<b>Synthesis and growth</b>				
$J_{tot}$	Total available C flux	-	$\mu g C d^{-1}$	Eq. (6)
$\mu$	Division rate of algae	-	$d^{-1}$	Eq. (7)
$r$	Growth rate of algae	-	$d^{-1}$	Eq. (8)
$Q_{CN}$	C:N mass ratio	5.68	$\mu g C (\mu g N)^{-1}$	[51]
$Q_{CP}$	C:P mass ratio	41	$\mu g C (\mu g P)^{-1}$	[51]

535

536

537

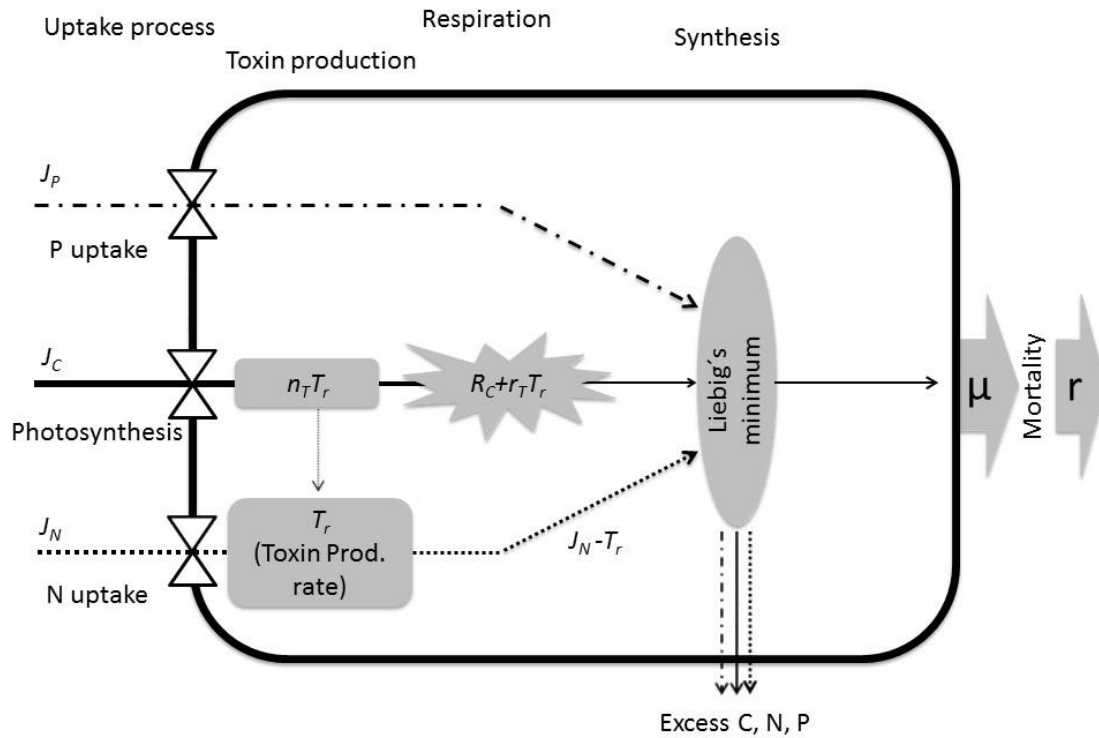
538

539

540

541

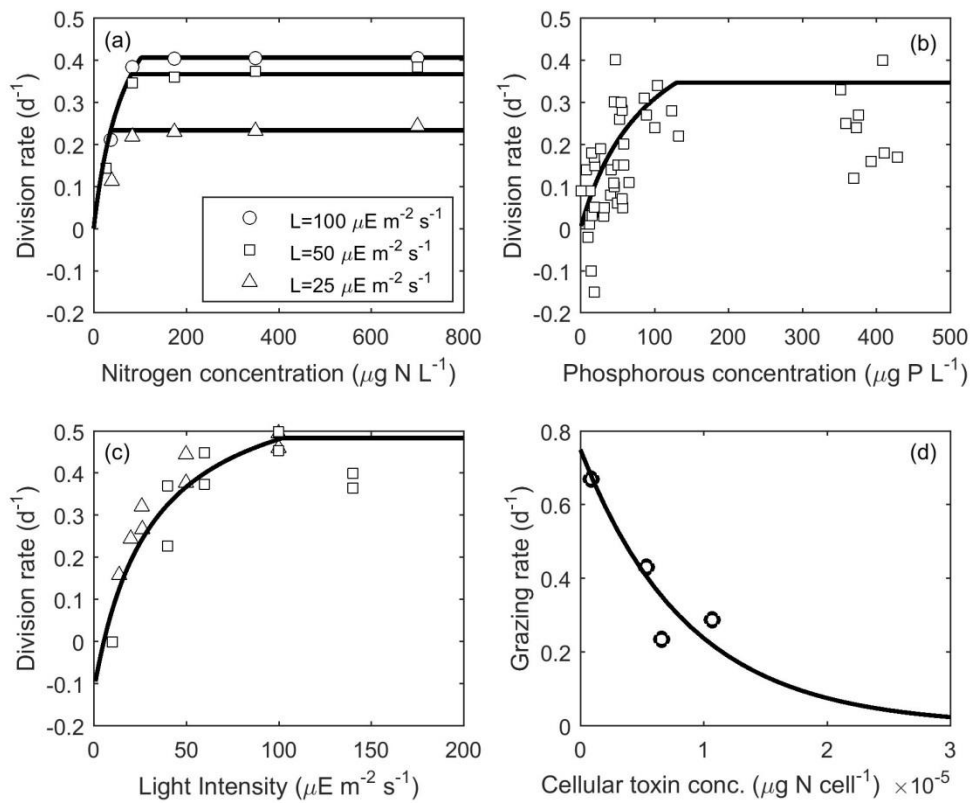
542   **Figures**



543

544 **Figure 1.** Schematic representation of the model showing how fluxes of nitrogen  
545 (dotted), carbon (solid) and phosphorous (dash-dot) are lost through respiration (gray  
546 explosion) and toxin production (gray rectangles), and combined (gray ellipse) to  
547 determine growth rate. White triangle symbols represent the functional responses for  
548 the uptake mechanisms.  $R_C$  represents the respiratory cost that includes the costs of  
549 both uptake and mobilization of resources for synthesis and the maintenance of  
550 structure. The rate at which toxin is synthesized from C and N is  $n_T T_r$ , and the  
551 respiratory cost of toxin production is  $r_T T_r$  where  $T_r$  is the toxin production rate. The  
552 ellipse represents synthesis of biomass from the available C, N and P following  
553 Liebig's law of the minimum and constrained by the Redfield ratio ( $\mu g C (\mu g N)^{-1}$   
554  $= 5.68$ ,  $\mu g C (\mu g P)^{-1} = 41$ ) [51]. In our steady state consideration, the excess amounts  
555 of assimilated C, N or P are assumed lost as excess resources.  $\mu$  represents the

556 division rate, and  $r$  is the population growth rate after subtracting predation mortality  
 557 from  $\mu$ .



558

559 **Figure 2.** Comparison of division rates ( $\mu$ ) between available data and model  
 560 outcome with the calibrated parameters by varying (a) nitrogen ( $P = 200 \mu\text{g P L}^{-1}$ )  
 561 (at three different light intensities  
 562  $L = 100 \mu\text{E m}^{-2} \text{s}^{-1}, 50 \mu\text{E m}^{-2} \text{s}^{-1}, 25 \mu\text{E m}^{-2} \text{s}^{-1}$  [52], (b) phosphorous ( $L =$   
 563  $45 \mu\text{E m}^{-2} \text{s}^{-1}, N = 200 \mu\text{g N L}^{-1}$  [53], and (c) light ( $N = 6000 \mu\text{g N L}^{-1}, P =$   
 564  $400 \mu\text{g P L}^{-1}$ ) [52, 54]. Grazing rate at different toxin concentrations (d). Data for  
 565 grazing on toxic *A. tamarense* strain CCMP 115 by *A. tonsa* were used [12].

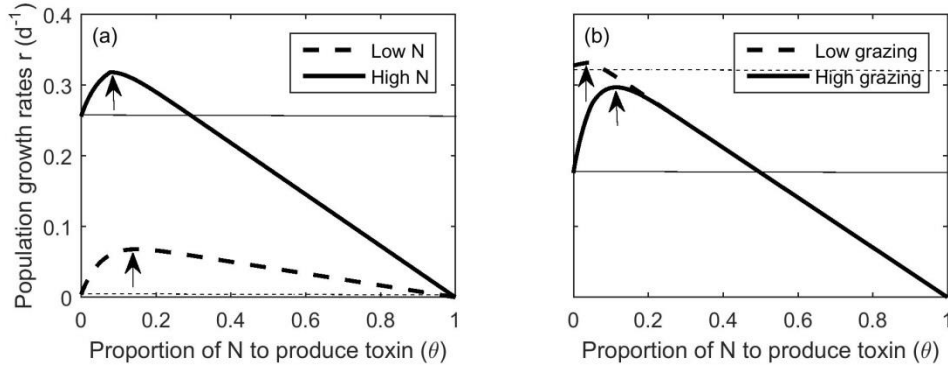
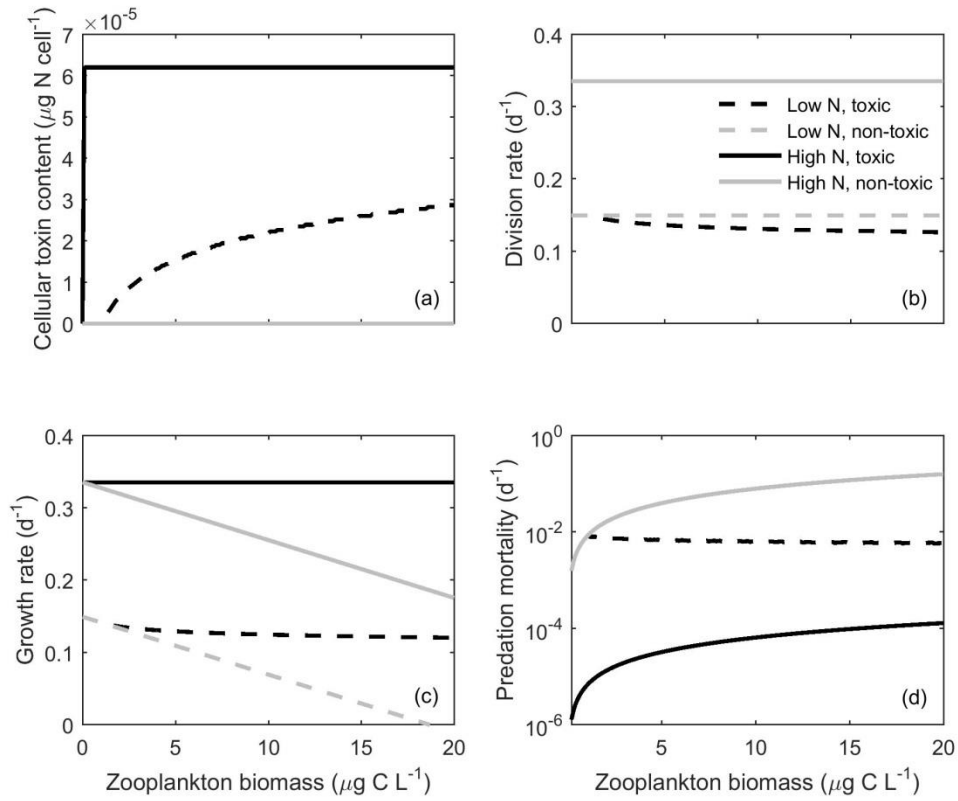


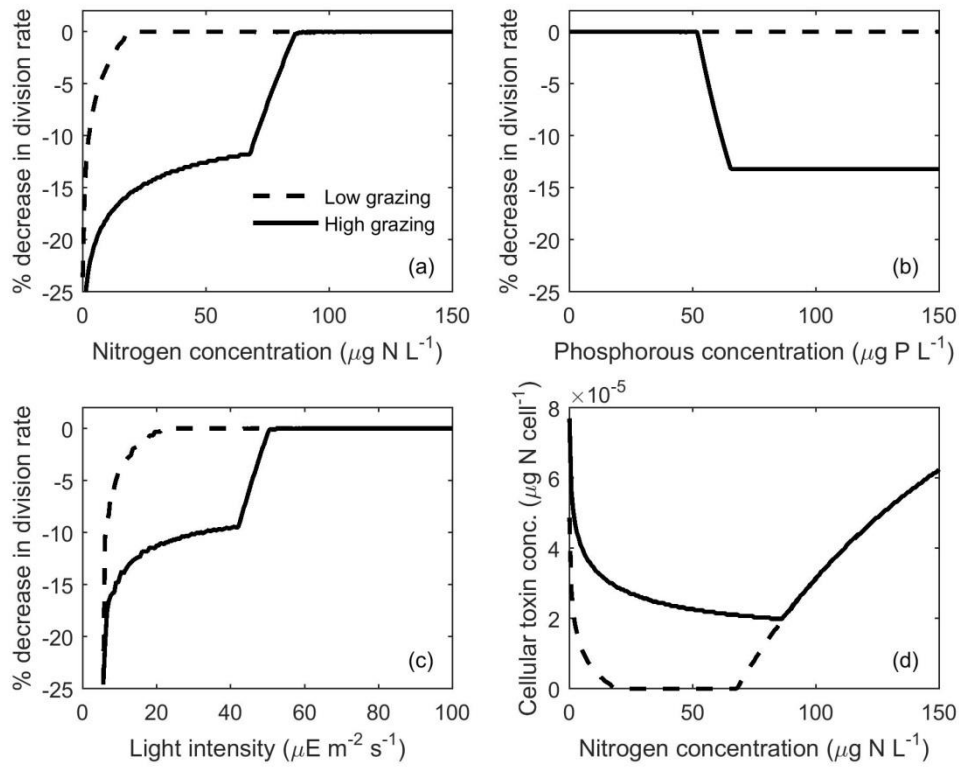
**Figure 3.** Population growth rate as a function of the fraction of assimilated nitrogen that is allocated to toxin production (a) at low and high environmental concentration of N ( $N=80 \mu\text{g N L}^{-1}$  and  $10 \mu\text{g N L}^{-1}$  with concentration of grazer  $Z = 10 \mu\text{g C L}^{-1}$ ), and (b) at high and low concentration of zooplankton ( $Z = 20 \mu\text{g C L}^{-1}$  and  $1 \mu\text{g C L}^{-1}$  with  $N = 75 \mu\text{g N L}^{-1}$ ). The maximum of the curves shows the optimal allocation strategy ( $\theta^*$ ) (marked by arrows). Thin lines represent growth rates in the absence of toxin production. Other resources are phosphate ( $P = 120 \mu\text{g P L}^{-1}$ , light intensity ( $L = 150 \mu\text{E m}^{-2}\text{s}^{-1}$ , and phytoplankton biomass ( $X = 90 \mu\text{g C L}^{-1}$ ).



575

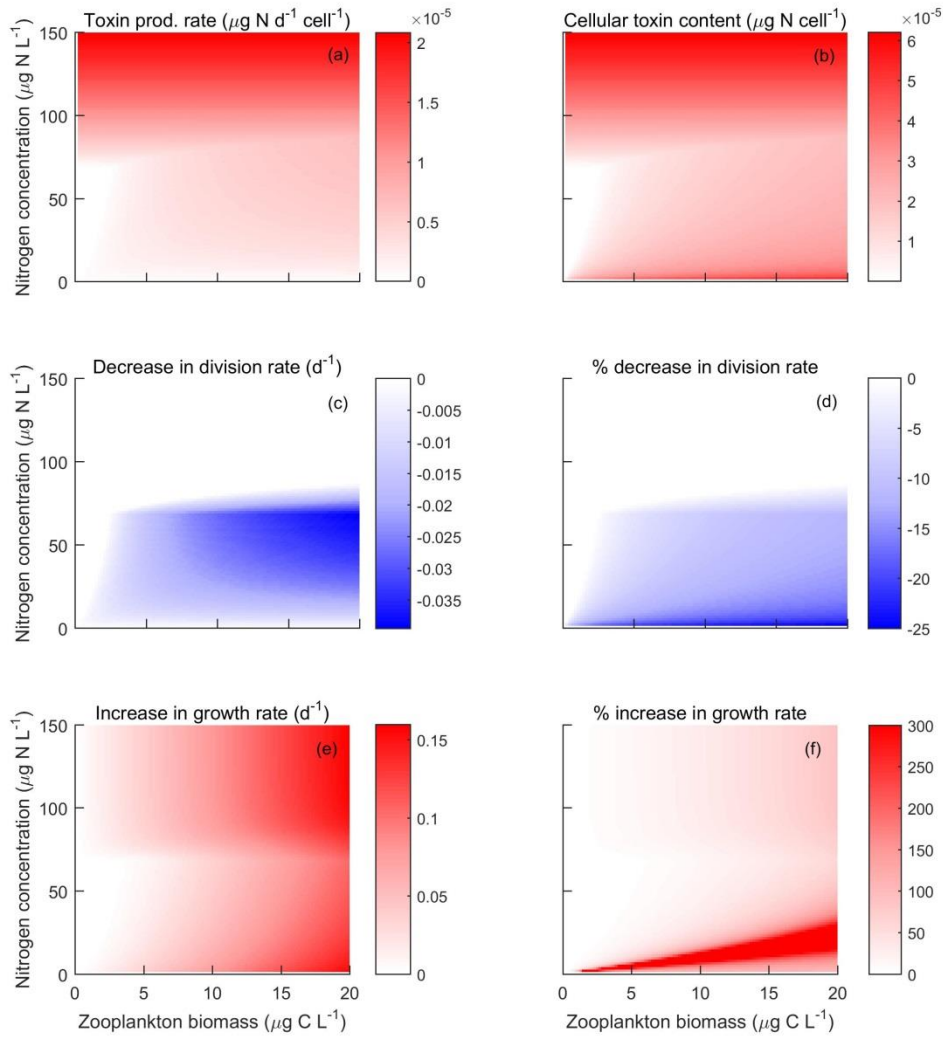
576 **Figure 4.** Optimal cellular toxin content (a), cell division rate (b), population growth  
577 rate (c), and predation mortality (d) as a function zooplankton biomass at low ( $N=20$   
578  $\mu\text{g N L}^{-1}$ ) and high ( $N=150 \mu\text{g N L}^{-1}$ ) N concentrations of defended (toxin producing)  
579 and undefended cells (non-toxic strain). Curves of division rates for defended and  
580 undefended cells under high N concentration lie on top of each other. Light intensity  
581  $L = 150 \mu\text{E m}^{-2}\text{s}^{-1}$  and phosphorous concentration  $P = 120 \mu\text{g P L}^{-1}$  in all plots.





582

583 **Figure 5.** Relative reduction in cell division rate as a function of nitrogen  
 584 concentration ( $L=150 \mu\text{E m}^{-2}\text{s}^{-1}$ ,  $P=120 \mu\text{g P L}^{-1}$ ) (a), phosphorous concentration  
 585 ( $L=150 \mu\text{E m}^{-2}\text{s}^{-1}$ ,  $N=40 \mu\text{g N L}^{-1}$ ) (b), and light intensities ( $N=120 \mu\text{g N L}^{-1}$ ,  
 586  $P=120 \mu\text{g P L}^{-1}$ ) (c) at high ( $Z=20 \mu\text{g C L}^{-1}$ ) and low ( $Z=1 \mu\text{g C L}^{-1}$ ) zooplankton  
 587 biomasses. Cellular toxin content as a function of N at high and low zooplankton  
 588 biomasses (d).



589

590 **Figure 6.** Surface plots of toxin production rate (a), and cellular toxin content (b), as  
 591 well as absolute and relative changes in cell division rate ( $\mu(\theta^*) - \mu(\theta = 0)$  and  
 592  $(\mu(\theta^*) - \mu(\theta = 0)) \times 100 / \mu(\theta = 0)$ ) (c, d), and population growth rates  
 593  $(g(\theta^*) - g(\theta = 0))$  and  $(g(\theta^*) - g(\theta = 0)) \times 100 / g(\theta = 0)$ ) (e, f) of defended relative  
 594 to undefended cells as a function of N-availability and zooplankton biomass. Light  
 595 intensity  $L = 150 \mu\text{E m}^{-2}\text{s}^{-1}$  and phosphorous concentration  $P = 120 \mu\text{g P L}^{-1}$  in  
 596 all plots.

597

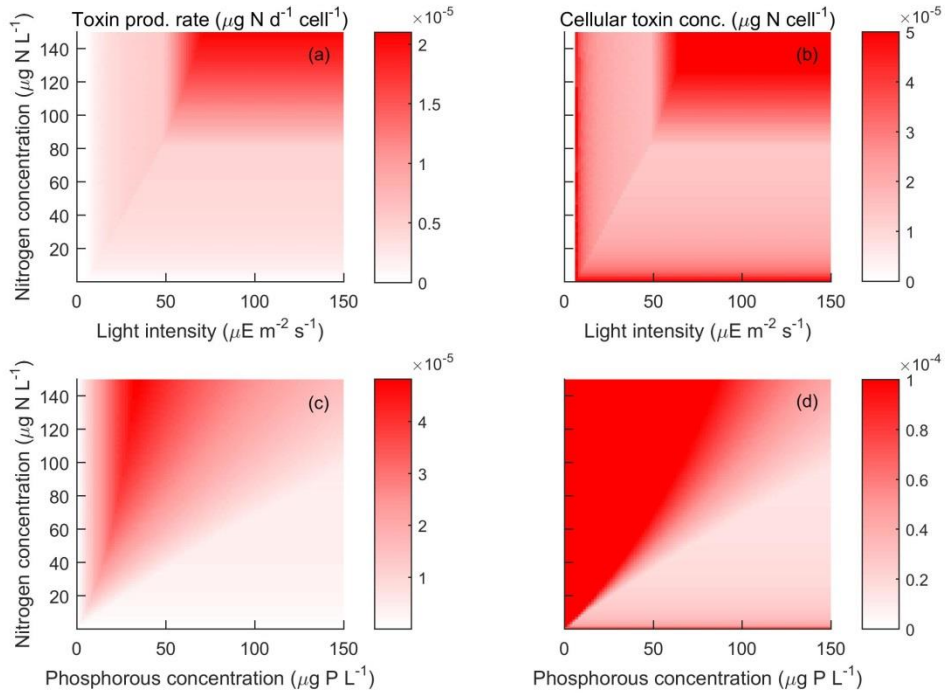


**Figure 7.** Surface plots of toxin production rate (a), and cellular toxin content (b) as a function of N-availability and light intensity. Zooplankton biomasses  $Z=10 \mu\text{g C L}^{-1}$ , and phosphorous concentration  $P=120 \mu\text{g P L}^{-1}$  in both plots. Surface plots of toxin production rate (c), and cellular toxin content (d) as a function of N and P-availability. Zooplankton biomasses  $Z=10 \mu\text{g C L}^{-1}$ , and light intensity  $L=150 \mu\text{E m}^{-2} \text{ s}^{-1}$  in both plots.

## Supplementary material

### Appendix A. Sensitivity analysis

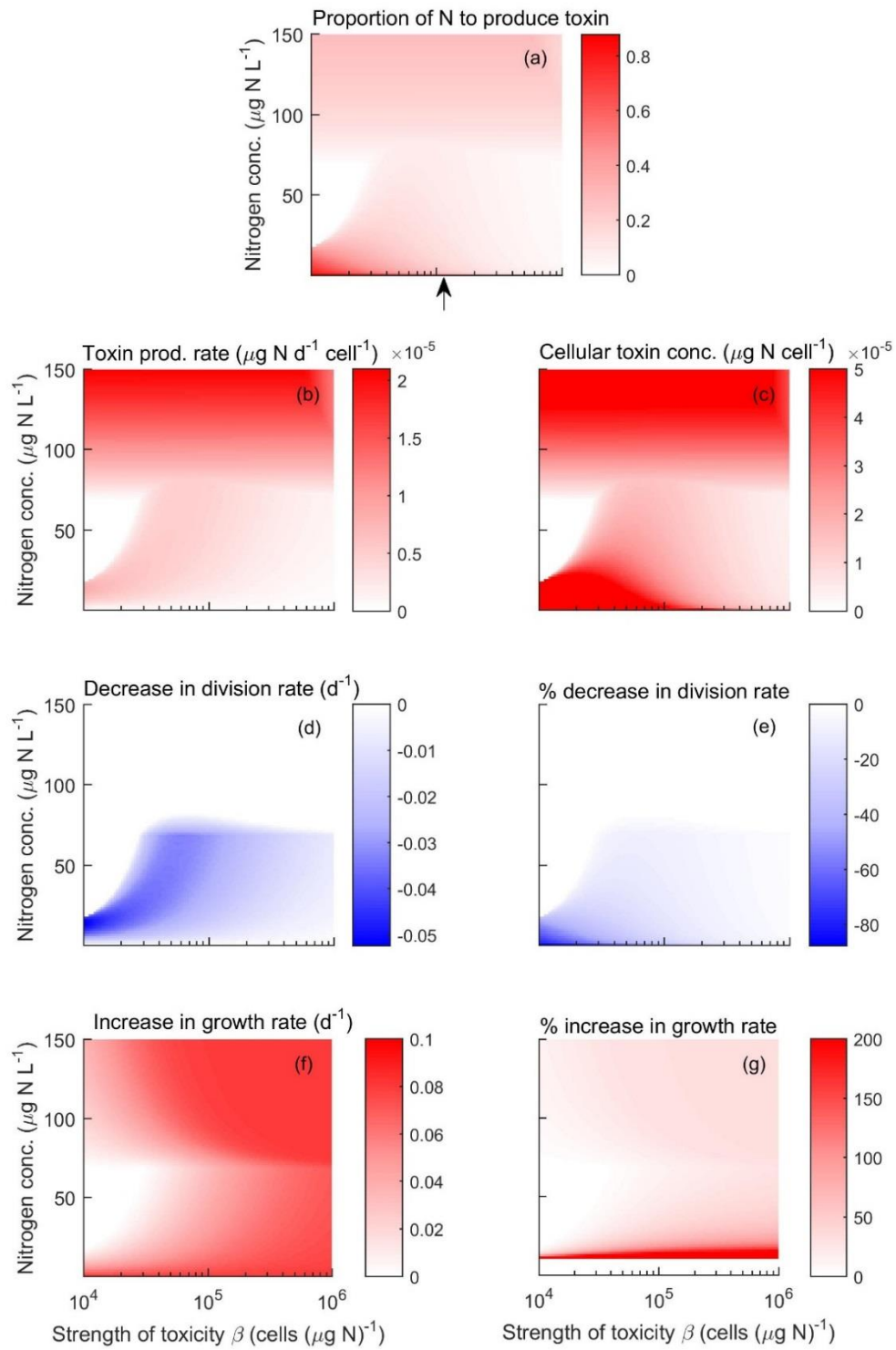
Fig. A1 shows the color plot with continuous variations in both N concentration and the benefit from toxin production ( $\beta$ ). The toxin production rate is high when the benefit from toxin production remains within certain range. However, it decreases at very high benefit range as organisms receive large benefit by producing small amount of toxin (Fig. A1b). As a result, benefits of toxin production in terms of population growth rate remains high when benefits are high and also N concentration is high.

Fig. A2 shows the color plot with continuous variations in both N concentration and the metabolic cost of synthesizing toxin ( $r_T$ ). When the cost is relatively low, an increase in N concentration increases toxin production (Fig A2b), as organisms get more benefit from toxin production rather than increasing division rate. However, when the toxin production is costly and N is sufficient in the system, organisms invest their energy in increasing division rate rather than production of costly toxin. Although, since low N does not support high growth, organisms produce toxin to increase their population growth rate in spite of their high cost.

635 **Figure legends**

636 **Figure A1.** Surface plots of optimal allocation of N to toxin production (a), toxin  
637 production rate (b), and cellular toxin content (c), as well as absolute and relative  
638 changes in cell division rate ( $(\mu(\theta^*) - \mu(\theta = 0))$  and  $(\mu(\theta^*) - \mu(\theta = 0)) \times 100 / \mu(\theta =$   
639  $0))$  (d, e), and population growth rates ( $(g(\theta^*) - g(\theta = 0))$  and  $(g(\theta^*) - g(\theta =$   
640  $0)) \times 100 / g(\theta = 0))$  (f, g) of defended relative to undefended cells as a function of N-  
641 availability and the strength of toxicity ( $\beta$ ). The position of arrow indicates the value  
642 of  $\beta$  used for other figures. The phytoplankton biomasses  $X=90 \mu\text{g C L}^{-1}$ ,  
643 zooplankton biomasses  $Z=10 \mu\text{g C L}^{-1}$ , light intensity  $L=150 \mu\text{E m}^{-2}\text{s}^{-1}$ , and  
644 phosphorous concentration  $P=120 \mu\text{g P L}^{-1}$  in all plots.

645 **Figure A2.** Surface plots of optimal allocation of N to toxin production (a), toxin  
646 production rate (b), and cellular toxin content (c) as well as absolute and relative  
647 changes in cell division rate ( $(\mu(\theta^*) - \mu(\theta = 0))$  and  $(\mu(\theta^*) - \mu(\theta = 0)) \times 100 / \mu(\theta =$   
648  $0))$  (d, e) and population growth rates ( $(g(\theta^*) - g(\theta = 0))$  and  $(g(\theta^*) - g(\theta =$   
649  $0)) \times 100 / g(\theta = 0))$  (f, g) of defended relative to undefended cells as a function of N-  
650 availability and the cost of toxin production ( $r_T$ ). The position of arrow indicates the  
651 value of  $r_T$  used for other figures. The phytoplankton biomasses  $X=90 \mu\text{g C L}^{-1}$ ,  
652 zooplankton biomasses  $Z=10 \mu\text{g C L}^{-1}$ , light intensity  $L=150 \mu\text{E m}^{-2}\text{s}^{-1}$ , and  
653 phosphorous concentration  $P=120 \mu\text{g P L}^{-1}$  in all plots.



654

655 Figure A1

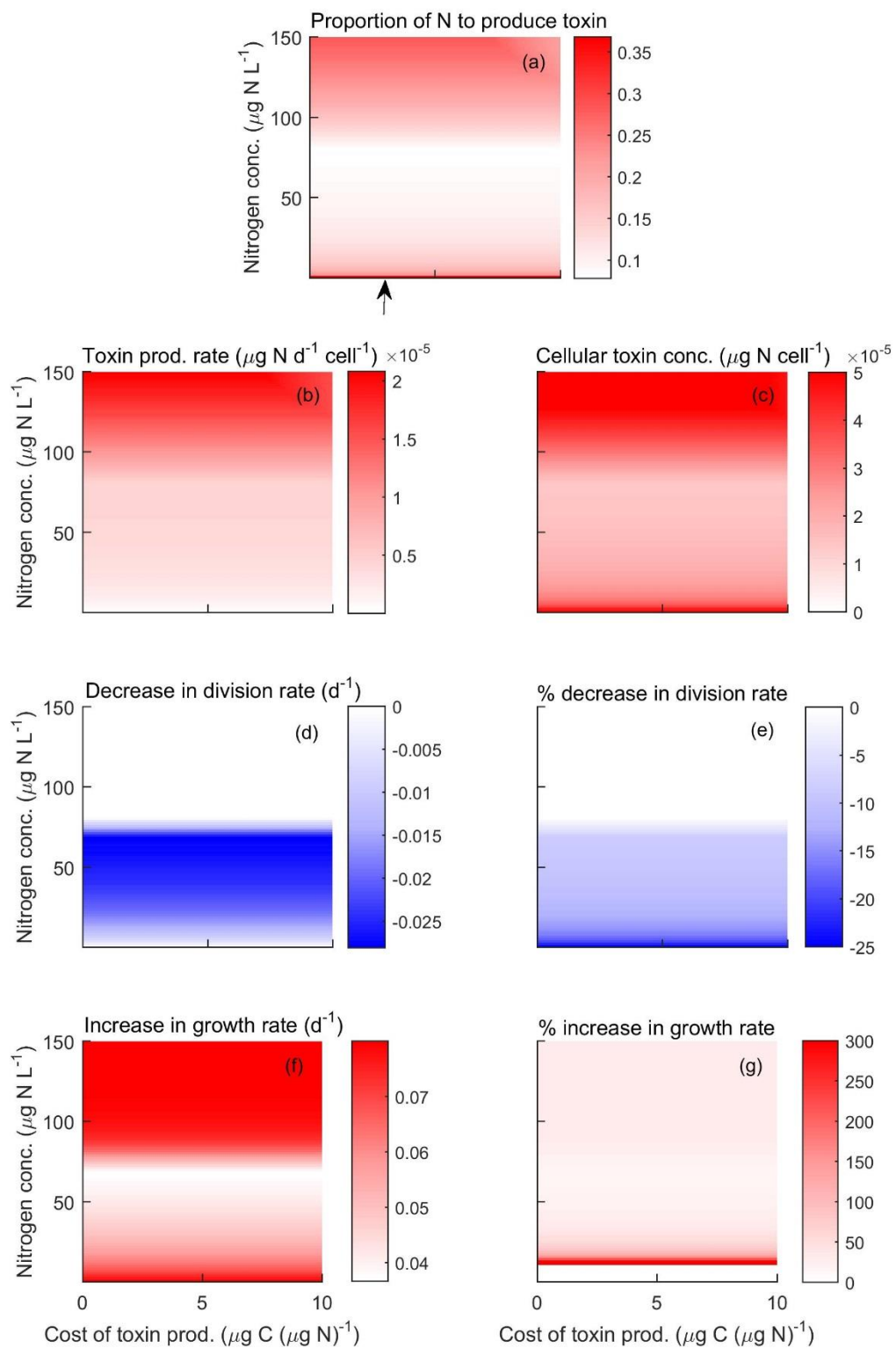


Figure A2